Abstract

Tropical Dry Forests (TDFs) are ecosystems with long drought periods, a mean temperature of 25^{o}C, a mean annual precipitation that ranges from 900 to 2000 mm, and that possess a high abundance of deciduous species (trees and lianas). What remains of the original extent of TDFs in the Americas remains highly fragmented and at different levels of ecological succession. It is estimated that one of the main fingerprints left by global environmental and climate change in tropical environments is an increase in liana coverage. Lianas are non-structural elements of the forest canopy that eventually kill their host trees. In this paper we evaluate the use of a Terrestrial Laser Scanner (TLS) in combination with hemispherical photographs (HPs) to characterize changes in forest structure as a function of ecological succession and liana abundance. We deployed a TLS and HP system in 28 plots throughout secondary forests of different ages and with different levels of liana abundance. Using a canonical correspondence analysis, we addressed how the VEGNET and HPs could predict TDF structure. Likewise, using univariate analysis of correlations we show how the liana abundance could affect the prediction of the forest structure. Our results suggest that TLS and HPs can predict differences in the forest structure at different successional stages, but that these differences disappear as liana abundance increases. Therefore, in well-known ecosystems such as the tropical dry forest of Costa Rica, these biases of prediction could be considered as structural effects of liana presence. This research contributes to the understanding of the potential effects of lianas in secondary dry forests and highlights the role of TLS combined with HPs to monitor structural changes in secondary TDFs.

1 Introduction

Lianas, woody vines, are a key structural component of tropical forests; they account for 25–40% of the woody stems and more than 25% of the woody species (*Schnitzer and Bongers, 2011*). Lianas are structural parasites that use trees to ascend to the forest canopies and move from tree to tree. Lianas have been defined as hyper-dynamic elements of the canopy structure (*Phillips et al. 2005, Sánchez-Azofeifa and Castro, 2006*). Lianas can be detrimental to host trees by competing with them for above- and belowground resources (*Chen et al., 2008*), reducing tree growth rates, and increasing tree mortality (*Schnitzer and Carson 2010*, *van der Heijden et al., 2013*).

In the last two decades lianas have increased in density and biomass in old-growth forests (*Phillips et al., 2002; Schnitzer and Bongers, 2011*), and this increment is considered to be one of the major structural changes in tropical forests (*Phillips and Lewis, 2014*). These structural changes mentioned above may have potential negative effects on carbon stocks since they tend to reduce carbon storage and uptake in old-growth tropical forests (*Durán and Gianoli, 2013; van der Heijden et al., 2015*). Liana dynamics in secondary forests and their impact on forest structure, however, are not yet understood despite the fact that secondary forests are becoming increasingly dominant in tropical regions, and currently occupy more area than old-growth forests (*Durán and Sánchez-Azofeifa, 2015; Wright, 2005*).

Lianas are considered light-loving plants, because they tend to respond positively to disturbance and show high density in areas of secondary forest succession (*Paul and Yavitt, 2011*). Furthermore, secondary forests may promote liana abundance because they provide both high light availability and an abundance of trellises (*Schnitzer and Bongers, 2002*). As

47 tree turnover increased gaps due to mortality, lianas can take advantage of this process and
48 form dense tangles, which in turn reduce the amount of light reaching the forest understory
49 (*Paul and Yavitt, 2011; Schnitzer et al., 2000*). These liana tangles can persist for long
50 periods (up to 13 years) and alter the successional pathway stalled by liana abundance by
51 inhibiting the regeneration, growth, and density of late successional species (*Schnitzer et al.,*
52 *2000*).

53 As of today, it is still unknown whether lianas can alter successional trajectories in
54 secondary forests resulting from anthropogenic disturbance (*Durán and Sánchez-Azofeifa,*
55 *2015*). Two studies in secondary wet forests have found an increment in liana density in the
56 first 20 years of regeneration (age since land abandonment), with a subsequent decline
57 (*DeWalt et al., 2000; Letcher and Chazdon, 2009*). This decline of lianas in wet forests
58 appears to be related with reductions in light availability due to greater tree and shrub
59 biomass at later stages of succession (*Letcher and Chazdon, 2009*). Nonetheless, it remains
60 unclear whether this pattern holds true with more open forest types, and whether other
61 factors such as structure, canopy openness, plant density and the volume of forest stands can
62 also influence successional trajectories of lianas (*Durán and Sánchez-Azofeifa, 2015;*
63 *Sánchez et al., 2009*).

64 Despite the fact of the important effect of lianas on the biomass distribution within
65 tropical forests (*Schnitzer and Bongers, 2011; Ledo et al. 2016*), and their potential role as
66 fingerprints of climate change (*Phillips et al. 2005*), remote sensing tools aimed to measure
67 their presence/absence as well as their distribution within tropical forests are limited (*Foster*
68 *et al., 2008, Kalacksa et al. 2007a & b, Zhang et al. 2006*). Current knowledge based on leaf
69 spectroscopy approaches provides two key messages regarding liana extent mapping: first

70 that lianas in tropical rainforests tend to confuse the spectral reflectance of their host trees
71 making it in many cases impossible to use remote sensing to create species maps (*Castro-*
72 *Esau et al., 2004)*, and second that there is a higher degree of probability of success for
73 efforts aimed to map liana coverage in tropical dry forests than on rain forests environments
74 (*Sanchez-Azofeifa et al., 2009b; Kalacska et al. 2007b)*. Moreover, studying the impact of
75 lianas on tropical dry forest structure, *Sanchez-Azofeifa et al*. (*2009*) used hemispherical
76 photography over a succession of tropical dry forests in Mexico, Costa Rica and Brazil,
77 found that lianas infested sites were significantly different in both canopy openness and
78 Woody Area Index (WAI).

79 Initial attempts aimed to start untangling the effects that lianas have on remote
80 sensing observations may require data fusion techniques on which hyperspectral remote
81 sensing approaches (leaf spectroscopy finding) are mergered with ground based forest
82 structure information derived from terrestrial laser scanners and hemispherical photography
83 (e.g. LAI, WAI and PAI). Terrestrial Laser Scanners (TLS) have demonstrated their
84 capability to measure canopy properties such as height and cover (*Ramírez et al., 2013*) and
85 tree architecture (*Lefsky et al., 2008*), (*Dassot et al., 2011*; *Richardson et al., 2014*). In the
86 last decade, there has been a rapid development in portable TLS (*Dassot et al., 2011;*
87 *Richardson et al., 2014*). When laser pulses emitted in the visible or near-infrared come into
88 contact with an object, part of that energy is reflected back toward the instrument which
89 triggers the recording of its distance and intensity (*Beland et al., 2014*). TLS systems
90 typically employ vertical and horizontal scanning around a fixed point of observation,
91 providing a hemispherical representation of biomass distribution in the forest -leaves,

92 branches and trunks- which allows for the exploration of foliage angle distributions and
93 clumping (*Clawges et al., 2007; Jupp et al., 2009; Strahler et al., 2008*).

94 Until today, there has been no concrete evidence about how liana abundance can
95 affect the prediction of the forest structure by TLS or hemispherical photographs (HPs),
96 which in turn can drive the development of better remote sensing techniques for mapping
97 their extent. Because of this, the objective of this study was to evaluate the feasibility of a
98 TLS named VEGNET in combination with HPs to assess changes in forest structure in
99 secondary TDFs with different levels of lianas abundance. The VEGNET is a TLS that
100 automatically scans a forest plot producing a vertical foliage density profile. Given its
101 automated mode of operation and semi-permanent installation, the VEGNET instrument is
102 described as an *in situ* Monitoring LiDAR (IML) (*Culvernor et al., 2014; Portillo-Quintero*
103 *et al., 2014*).

104 As such, in this paper we first assess the changes of tropical dry forests structure due
105 to liana presence and forest succession. Second, we analyze the potential of VEGNET and
106 HPs to detect the vertical structure of forest stands at different successional stages. Finally,
107 we examine how liana abundance could affect the bias of prediction of VEGNET and HPs to
108 detect the level of succession of a given forest stand. Therefore, in well-known ecosystems
109 such as the tropical dry forest of Costa Rica, this bias of prediction could be considered as
110 the effect of liana presence on forest structure.

111

112 **2 Methods**

113 **2.1 Study Area**

114 The study area is located in the Santa Rosa National Park Environmental Monitoring Super
115 Site (SRNP-EMSS), which is a part of the Guanacaste Conservation Area in Costa Rica
116 (10°48" N, 85°36" W) (Figure 1). This site covers an area of 50,000 ha, receives 1720 mm
117 of annual rainfall, has a mean annual temperature of 25°C and a 6-month dry season
118 (Dec–May) (*Kalácska et al.,2004*). The SRNP-EMSS site has suffered intense deforestation
119 in the past 200 years due to the expansion of pasturelands (*Calvo-Alvarado et al., 2009*).
120 Original land management practices in the park included pasture rotation between different
121 large corrals surrounded by life fences that can still be identified today. More recently (early
122 1970's) with the creation of Santa Rosa National Park, a process of secondary regeneration
123 has become the dominant land cover change force in the region. Today and after the creation
124 of SRNP, the uplands of the park are a mosaic of secondary forest in various stages of
125 regeneration and with different land use histories related with anthropogenic fires, intense
126 deforestation, and clearing for pasture lands (*Kalácska et al., 2004; Arroyo-Mora et al.,*
127 *2005a, Cao et al, 2015*).
128
129 **2.2 Definition of forest cover and plot age.**
130 A map of forest cover and forest cover ages was generated using aerial photographs
131 collected by the US Army in 1956 (Scale 1:24,000), a Multispectral Scanner (MSS) image
132 from 1979 (80 m spatial resolution); 4 Landsat Thematic Mapper [TM] images from 1986,
133 1997, 2000 and 2005 (28.5 m spatial resolution); one Spot Multispectral image from 2010
134 (20 m spatial resolution); and a Landsat 8 image from 2015. All images had less than 10%
135 cloud cover.

136 The 1986 image was georeferenced to 1:50,000 topographic maps from the Costa Rica
137 National Geographic Institute with a Root Mean Square Error (RSME) of 0.5 pixels or 14.25
138 m. We defined this as our master image in order to georeference all of the other images, as
139 such all other images were then geo-referenced to the 1986 image seeking a RMSE close to
140 0.5 pixels between the master and the target image. All images where then classified using a
141 supervised classification. Image accuracy was conducted for the 1997, 2000, 2005 and 2010
142 satellite images as part of independent validation efforts conducted by the Costa Rica's
143 National Forest Financing Fund (FONAFIFO). Overall accuracy for the forest/non-forest
144 images was 90%. Further information on image processing can be found in Sánchez-
145 Azofeifa et al. (2001).
146 Final quality controlled forest cover maps (forest non-forest) for 1956, 1979, 1986, 1997,
147 2000, 2005, 2010 and 2015 were cross referenced to produce a tropical dry forest age map.
148 Specifically, forest coverage with 60 years old correspond to woodlands which were being
149 observed in images since 1956; forests that were 40 years old were not detected in 1956 but
150 have been recognizing as forests since 1979; on the other hand, woodlands that were referred
151 to as being 10 years old have a minimum of 10 years as a discriminable forest coverage.
152 Based on Arroyo-Mora et al. (2005b) and Kalascka et. al's (2005a) studies the following
153 successional classification was developed: Ages 10 to 40 years (Early), and ages 40 to 60
154 (Intermediate). Figure 1 presents the final land cover and forest age map for our study area.
155

156 **2.3 Plots selection and description**

157 Based on Figure 1, twenty-eight randomly stratified 0.1ha plots were selected. The number
158 of plots chosen for each forest successional stage was based upon each stages total forest cover

159 area. Plot sizes of 0.1 ha follows convention used in tropical forest studies at this site (Kalascka
160 et al. 2005a). Fieldwork conducted in July 2016 was conducted in order to characterize
161 diameter at breast height (DBH), tree height, total biomass, VEGNET observations (canopy
162 vertical profiles) and hemispherical photos (Canopy openness and Leaf Area Index).
163 The characterization of successional stages was performed following previous approaches
164 for seasonally dry forests of Costa Rica (*Arroyo-Mora et al., 2005b; Kalácska et al., 2005*) and
165 adjusted according to the estimated forest ages (Figure 1). These approaches categorized the
166 secondary regeneration in different successional stages such as early and intermediate
167 successional stages (*E* and *I*, respectively) (*Arroyo-Mora et al., 2005a*). The *E* stage is a
168 forest area with patches of sparse woody vegetation composed of shrubs, small trees, and
169 saplings, with a thick herbaceous understory, and with a single stratum of tree crowns with a
170 maximum height of less than 10 m (*Castillo et al., 2012*). Some of the common species that
171 are characteristic of this early stage of succession includes *Genipa americana*,
172 *Cochlospermum vitifolium*, *Gliricidia sepium*, *Randia monantha* (*Hilje et al., 2015;*
173 *Kalácska et al., 2004*). In contrast, the *I* stage has two vegetation strata composed of
174 deciduous species of woody plants. The first strata is comprised of fast-growing deciduous
175 tree species that reach a maximum height of 10–15 m (e.g., *Cydista aequinoctialis*) and the
176 second stratum is represented by lianas and vines, adults of shade-tolerant and slow-growing
177 evergreen species as well as the juveniles of many species such as *Annona reticulata*,
178 *Ocotea veraguensis*, and *Hirtella racemosa* (*Arroyo-Mora et al., 2005a; Kalácska et al.,*
179 *2004*). No lianas were present in the early successional stage plots. Lianas abundance tends
180 to increase in early forests during their transition to intermediate stages. We did not select
181 "late forests" at our study site since they tend to reflect structural characteristics (DBH, three

182 height and species composition) associated with tropical moist forest (Tosi, personal
183 communication).
184 On the other hand, the characterization of the plots according to the liana abundance was
185 based on the structure of plants that compose the tropical dry forest of SRNP-EMSS. In this
186 way, we classified the 28 plots according to the relative abundance of stems of lianas over
187 total number of stems, where plots with a relative abundance greater than 0.1 were
188 categorized as plots having high liana abundance (HL), while plots with a relative
189 abundance lower than 0.1 were categorized as having a low liana abundance (LL). Although
190 this classification seems to be in-deterministic, this kind of classification represents an
191 important ecological component which is very difficult to study as a continuum due to its
192 spatial and temporal variation, and its categorization can help to improve the understanding
193 of ecological processes as many other ecological categories.
194 At the end of this characterization, ours plots for the study consisted of 5 *E*-LL plots, 6
195 *E*-HL plots, 7 *I*-LL plots, and 10 *I*-HL plots. In each of these plots we extracted all the
196 information available to describe the dry forest according to its structure, but at the same
197 time deployed the ground LiDAR and hemispherical photograph measurements to predict
198 and describe that structure. Information about the parameters used and estimated according
199 to the forest structure, ground LiDAR, and hemispherical photographs is described below.
200
201 **2.4 Forest structure**
202 Four parameters that characterize the forest structure were used in this study. These
203 parameters were selected because these are easily obtained in any forest inventory, which
204 could help in the applicability of this study in other regions. Specifically, we selected the

205 stem density (stems/ha) as a parameter to describe the number of individuals per plot, the
206 mean diameter at breast height (1.3 m) (DBH_{mean}, cm) as a parameter that can describe the
207 mean size of the individuals, the total basal area (TBA, m^2) as a parameter that can describe
208 the biomass of each plot, and the ratio of liana basal area to TBA (L/TBA) as a parameter
209 that can describe the contribution of lianas biomass to the total biomass of each plot. Each of
210 these parameters was extracted from DBH measurements for lianas (>2.5 cm) and trees (>5
211 cm).
212
213 **2.5 Ground LiDAR measurements**
214 The VEGNET ground LiDAR system was deployed in the middle of each of the selected
215 plots, in which a single successful scan was performed between June 12th to June 27th, 2016.
216 The VEGNET IML instrument uses a phase-based laser rangefinder with a wavelength of
217 635 nm, in which a laser beam is directed at a rotating prism that reflects the laser at a fixed
218 angle of 57.5° zenith or the "hinge angle" (*Jupp et al., 2009*). The prism is designed to
219 perform full 360° azimuth rotations at this fixed zenith angle (no vertical scanning motion)
220 and has the capability to be programmed to obtain up to 7360 range measurements for a full
221 azimuth scan (an average of 20.6 measurements per azimuth degree) (*Culvenor et al., 2014*).
222 Because sunlight irradiance may cause interference with the VEGNET laser at the same
223 wavelength (*Culvenor et al*., 2014, *Portilllo-Quintero et al*., 2014), measurements for the
224 VEGNET were conducted at night. Some tests of the measurement process by VEGNET at
225 night time indicated that at distances greater than 60 m or in areas larger than 3600 m^2 (0.36
226 ha) the laser beam does not provide reliable measurements (*Culvenor et al., 2014*). In a
227 tropical forest setting, data analysis and interpretation may be restrained to the footprint,

228 which is dependent on forest height at each site. Based on the forest heights of our study
229 sites, the effective footprint of LiDAR measurements was within 0.1ha of our original
230 sampling area.

231 From these measurements at night six parameters were estimated: the maximum tree
232 height (H_{max}), the plant area index (PAI), plant area volume density (PAVD), the centroid of
233 x (C_x) and y (C_y), and the radius of gyration (RG). To estimate these parameters, the height
234 (h) was initially calculated as the cosine of the laser zenith angle (57.5°) multiplied by the
235 laser distance measurement (d) assuming that the terrain is flat as describe *Culvenor et al.*
236 (*2014*).

237 On the other hand, canopy "hits" and "gaps" were recorded to enable the calculation
238 of angular gap fraction or gap probability (P_{gap}) at each h where a leaf, trunk or branch was
239 hit by the laser (*Lovell et al., 2003*). P_{gap} at a given h is the ratio of the number of valid
240 returns below z ($\#z_i < h$) to the total number of laser shots (N) (*Culvenor et al., 2014*):
241
242 $$P_{gap(z)} = [\#z_i < h\ ] / N \quad (1)$$
243
244 Consequently, the estimation of cumulative plant area index (PAI) by the conversion of
245 $P_{gap(z)}$ was performed using the following the equation (*Culvenor et al., 2014*):
246
247 $$PAI_{(z)} = -1.1 \times \ln(P_{gap(z)}) \quad (2)$$
248

From this calculation, the density of vegetation components at any level of z was computed as the derivative of PAI with respect to h. This calculation is commonly referred to as the plant area volume density (PAVD) (*Culvenor et al., 2014*) described by:

$$PAVD_{(z)} = \delta\, PAI_{(z)} / \delta_z \quad (3)$$

It is important to note that these calculations represent tridimensional variations (x, y, z) of the forest structure (*Culvenor et al., 2014*), because of this, in our statistical analysis we used the maximum h estimated by the LiDAR per plot (H_{max}), the cumulative PAI as a function of the canopy height (PAI), and the mean PAVD at different heights ($PAVD_{mean}$). These calculations were extracted using the "VEGNET Data Display and Export Version 2.5" software developed by Environmental Sensing Systems Inc (Melbourne, Australia).

Likewise, from the LiDAR measurements we also used shape metrics such as the centroid (C) and radius of gyration (RG) to understand how the vertical profile of the forest could change according to successional stages and liana abundance. The RG and the C are metrics that are mainly used in LiDAR waveforms to describe the motion of objects and the manner in which material is distributed around an axis (*Muss et al., 2013*). We used a similar approach by calculating the C and the RG for the PAVD vertical profile of each plot. Specifically, C represents the geometric center of a two-dimensional (x and y) region (e.g., the arithmetic mean position) of all the points (n) in the shape of the PAVD profile and it could, specially, be interpreted as the variability of PAI with height and it will change as a function of understory changes along the path of succession (grasses to shrubs to short

trees). On the other hand, RG is the root mean square of the sum of the distances for all points on the PAVD vertical profile, which is described as:

$$RG = \sqrt{\frac{\sum(x_i - C_x)^2 + \sum(y_i - C_y)^2}{n}} \quad (4)$$

This parameter can be visualized as the relationship between the total length of the PAVD vertical profile and its shape and position, which are determined using the sum of *x* or *y* coordinates divided by the total length of the profile (*Muss et al., 2013*). In general, the RG captures the manner in which the PAVD profile is distributed around the centroid, making it a better descriptor of the vertical profile shape than just the centroid itself, and thus, more suitable for relating VEGNET measurements to forest structure (*Muss et al., 2013; Culvenor et al., 2014*). Therefore, we used the RG to relate the shape of the PAVD profile to forest biomass at the footprint level For a more detailed explanation on the functioning of the VEGNET in the field please refer to *Portillo-Quintero et al*. (*2014*) as well as *Culvenor et al.* (*2014*). A single successful scan was performed during the wet season using the VEGNET instrument at each site on clear nights.

2.6 Hemispherical photographs

Hemispherical photographs (HPs) were taken during the early morning in the middle of each plot, using a digital camera (E4500, Nikon, Tokio, Japan) equipped with a fisheye lens of 35 mm focal length. The camera was leveled at 1.50 m by a tripod and orientated towards magnetic north, in order to ensure photographic standardization. The resulting pictures were analyzed using the software Gap Light Analyzer version 2.0.4 (*Frazer et al., 1999*). This

294 analysis was performed by creating 340 sky sectors (36 azimuth classes and 9 elevation
295 angle classes) with a time series of 2 min along the solar track. The leaf area index (LAI)
296 and the canopy openness were subsequently extracted by this analysis; however, the LAI
297 was extracted using the "4 ring" (with a zenith angle between 0 to 60º) which is a more
298 accurate depiction of the site than using "5 rings" because the latter takes into account trees
299 that are not immediately surrounding the site, and which are found outside of the plot
300 footprint.
301
302 **2.7 Statistical analysis**
303 This study compared the effect of the successional stages, the abundance of lianas, and their
304 interaction on the parameters of forest structure as well as VEGNET-HPs parameters using a
305 multivariate analysis of variance (MANOVA), in order to demonstrate that this study had
306 been conducted in contrasting environments. For each MANOVA we extracted the
307 univariate analysis of variance (ANOVA) to describe the multivariate effects of each
308 parameter. To show the potential of the VEGNET and HPs to predict variations in the
309 structure of the dry forest, we applied a canonical correlation analysis (CCA) using the
310 VEGNET-HPs parameters as independent variables and the features of the forest stand as
311 dependent variables. Due to the CCAs sensitivity to the collinearity among variables (*Quinn*
312 *and Keought, 2002*), we only used RG, PAI, $PAVD_{mean}$, H_{max}, LAI, and canopy openness as
313 independent parameters. Specifically, the CCA was used to extract the canonical correlation
314 between VEGNET-HPs and forest structure (eigenvalues), the correlation between the
315 canonical variates and each matrix (eigenvectors), and the scores that describe the
316 multidimensional variation of each plot according to its correlation. To extract the statistical

317 significance of the canonical correlation coefficients, we computed an asymptotic test on the
318 first canonical dimensions to extract the *F*-approximations of Wilks' Lambda along with its
319 significance. This statistical significance was subsequently validated using a permutation
320 test on each dimension by 10000 iterations.

321 After describing the potential of the VEGNET-HPs parameters to predict variations
322 in the structure of the dry forest, we were interested in demonstrating how the relative
323 abundance of lianas could affect the bias of prediction extracted from these sensors. In
324 ecological terms, it is a perceived expectation that during successional transitions increases
325 in basal area, height and vertical strata of the vegetation should be observed; consequently,
326 these transitions could be translated into increases in VEGNET-HPs parameters (except
327 canopy openness which is inverse). However, from hypothesis derived from previous
328 studies, it is possible that the abundance of lianas may actually arrest the forest succession
329 and reduce the biomass accumulation of woody vegetation (*Paul and Yavitt 2011; Schnitzer*
330 *et al., 2000*). If the above is true, correlations between descriptors of forest structure and
331 parameters extracted from VEGNET and HPs could be diffuse or stochastic in the dry forest,
332 and their application under the presence of lianas could prove ineffective. Under this
333 reasoning, we compare the parametric correlations of four parameters according to the
334 successional stages and the liana abundance, separately. The four parameters selected were
335 those with the two highest correlation values for the VEGNET-HPs matrix and the two
336 parameters with the highest correlation values for forest structure, determined by the first
337 two canonical dimensions described by the CCA. This comparison was conducted using an
338 ordinary resampling method to replicate the correlation 5000 times, in which the resampled

values were used to build density plots to describe the bias of prediction according to its overlap.

The previous analyses were conducted in R software version 3.3.1 (R Development Core Team, 2016) using the "CCA" package (*González and Déjean, 2015*) to extract the canonical correlations, the "CCP" package (*Menzel, 2009*) to extract the significance of the CCA and its permutation, and the "boot" package (*Canty and Ripley, 2016*) to extract the resampled values. When the normality of the data was not reached, each parameter was previously transformed using the Box-Cox transformation for the analysis.

3 Results

3.1 Changes on forest structure along the path of succession and liana abundance

According to the MANOVA, the forest structure of our plots differed between successional stages (Wilk's $Lambda_{(4,21)} = 0.51$; $p < 0.01$) and liana abundance (Wilk's $Lambda_{(4,21)} = 0.58$; $p < 0.05$), but without interaction between these categories (Wilk's $Lambda_{(4,21)} = 0.76$; $p = 0.20$). This analysis suggests that the DBH_{mean} and TBA were the only parameters affected by the interaction between successional stages and liana abundance, where *E* successional plots with LL and *I* plots with HL showed lower values of DBH_{mean} and TBA than *E* and *I* plots with HL and LL, respectively (Table 1). In terms of the effect of the liana abundance, the univariate analysis suggests that plots with LL showed lower values of L/TBA in comparison with HL plots.

3.2 VEGNET-Hemispherical Photographs (HPs), forest succession, and liana abundance

362 The multivariate comparisons of the VEGNET-HPs parameters showed that the sensor
363 estimations did not differ between successional stages (Wilk's $Lambda_{(8,17)} = 0.58$; $p =$
364 0.21), liana abundance (Wilk's $Lambda_{(8,17)} = 0.62$; $p = 0.29$), and these categories did not
365 show an interaction (Wilk's $Lambda_{(8,17)} = 0.53$; $p = 0.14$). Despite the absence of a
366 multivariate effect of the liana abundance, the univariate responses extracted from this
367 comparison suggest that the LAI and canopy openness differs between plots with HL and
368 LL, where LL plots showed lower values of LAI and higher values of canopy openness in
369 comparison with HL plots (Table 2). On the other hand, the univariate responses showed
370 that the canopy openness was affected by the successional stages, where *E* successional plots
371 showed higher values of canopy openness than *I* plots. Likewise, the univariate comparisons
372 suggest that C_x, PAI, and $PAVD_{mean}$ are affected by the interaction of the successional stages
373 and liana abundance, where *E* successional plots with LL and *I* plots with HL showed higher
374 values of C_x, PAI, and $PAVD_{mean}$ in comparison with *E* and *I* successional plots with HL and
375 LL, respectively.
376
377 **3.3 Canonical correspondence analysis and trends of forest structure**
378 The CCA showed that sensor parameters are strongly associated with the trends in forest
379 structure (Fig 2). In general, the first and second canonical dimension showed correlations of
380 0.81 (Wilk's $Lambda_{(24,64.01)} = 0.13$; $p < 0.01$) and 0.72 (Wilk's $Lambda_{(15,52.85)} = 1.46$; $p =$
381 0.16) between our sensors and forest structure. Specifically, the correlation between the
382 canonical variates in the first canonical dimension suggested that canopy openness and the
383 LAI have a great weight in the sensor matrix, while L/TBA and stem density had an
384 important effect on the forest structure (Fig 2a). Likewise, the correlation between the

canonical variates in the second canonical dimension showed that H_{max} and $PAVD_{mean}$ had a strong correlation with the sensor parameters, while TBA and steam density had a strong correlation on the forest structure. The scores that described the multidimensional variation of each plot did not reflect a visual aggregation according to the successional stages and liana abundance (Fig. 2b). In terms of the validation of the significance of the canonical correlation coefficients, the permutations test showed that there is an important increase in the significance of the first two canonical dimensions (Fig. 2c, 1d), where the first dimension presented an increase of 0.21 points for the Wilks's statistic, while the second dimension showed an increase of 0.25 points, which results in a significant effect.

3.4 Comparison of correlations between successional stages and liana abundance

The different trends of correlation showed that the successional stages and mainly the liana abundance have an important effect in the prediction of the forest structure using VEGNET-HPs parameters (Figure 3), but at the same time, these trends showed that some of these parameters have the potential to predict the implication of the liana abundance on the forest structure. Specifically, variation in the correlations of canopy openness on L/TBA (Figures 3a, b, c) and H_{max} on TBA (Figures 3g, h, i) showed that the correlation trends between successional stages are overlapped, while the correlations trends between liana abundance are separated, in where low values of canopy openness and H_{max} are associated with high values of L/TBA and TBA, and consequently with the discrimination of HL plots. Likewise, variation in the correlation between LAI and L/TBA showed that the trends might not be used to separate successional stages or liana abundance (Figures 3d, e, f). However, the correlation between H_{max} and TBA suggest that H_{max} can not discriminate between different

408 successional stages, but can discriminate different liana abundance since lower values of
409 correlation are associated with HL plots (Figures 3j, k, l).
410
411 **4 Discussion**
412 **4.1 Potential of VEGNET and HPs to detect the vertical structure of forest stands at**
413 **different successional stages**
414 Woody vines or lianas tend to proliferate in disturbed forest stands such as regenerating
415 forests (*Paul and Yavitt, 2010*). Much research on liana ecology, however, has focused on
416 old-growth forests despite that secondary forests currently cover a larger area than old-
417 growth forests and may become the dominant ecosystem in tropical regions (*Wright, 2005*).
418 Due to shorter stature and a higher variability of light in secondary forests, lianas may be
419 particularly abundant in these ecosystems, but little is understood about the role of lianas in
420 forest succession (*Letcher and Chazdon, 2009*). In this study, we used the VEGNET, a
421 terrestrial LiDAR system combined with HPs, to assess the impact of liana abundance on
422 forest succession. Our overall analysis indicated that VEGNET parameters, in combination
423 with HPs derived information, were able to characterize changes in forest structure at
424 different successional stages with and without lianas. Changes observed using HP, along the
425 successional gradient, we similar to those observed in other tropical dry forests
426 environments where parameters such as biomass, LAI, canopy openness and H_{max} changed
427 as trees grow (*Sanchez-Azofeifa et al. 2009*). Our work using the TLS suggested also that
428 this technology can be also used to detect differences along the forest succession trajectory
429 when lianas are integrated into the analysis. In terms of the comparison of VEGNET
430 parameters between our categories, probably the effect of the interaction of the successional

stages and liana abundance on C_x, PAI and $PAVD_{mean}$ are some of the most reveling. As lianas emerge along the path of succession they create a more heterogeneous space which is captured by the variability on C_x. C_x is affected by PAI and $PAVD_{mean}$ as function of understory components (shrubs, grasses and also liana tangles). A higher value of C_x may be interpreted on an E-LL as a high dominance of shrubs, tall grasses and short trees; while a high value of C_x on a E-HL will mean a high density at low height of tangles combined with shrubs which makes accessibility impossible to some sites due to a high density of understory liana tangles.

4.2 How liana abundance could affect the bias of prediction of VEGNET and HPs to detect the level of succession of a given forest stand?

When we consider the bias of correlations between the forest structure and the parameters extracted from our two sensors at different successional stages, as well as liana abundance, our results suggest that this latter variable has an important effect on the bias of prediction for a given forest structure. The main reason is probably a result of lianas introducing random tangles into the 3-dimensional space that is occupied by all forest biomass at a given plot. In other words, lianas tend to randomize or reduce the degree of organization of the natural space which is typically utilized by trees. This randomization of the 3D space occupied by trees and lianas is an element that has not been considered as of today; since most studies do not consider the space occupied by lianas because of a lack of TLS information.

This change in deterministic patterns of the forest structure is probably due to competition between lianas and trees in forest stands within a random 3D space. In disturbed

454 sites, such as secondary forests, lianas deploy leaves in the canopy and create large amounts
455 of tangles in both the ground and mid canopy, this high density of tangles contribute to a
456 reduction on the amount of available transmitted incoming solar radiation available for
457 photosynthesis at the understory (*Sanchez-Azofeifa et al. 2009, Graham et al., 2013*).
458 Moreover, in regenerating stands within forests (e.g., treefall gaps), high densities of lianas
459 can inhibit the regeneration of tree species and reduce the abundance of shade-tolerant trees
460 (*Schnitzer et al., 2000*), which in turn can affect the 3D arrangement of species within a
461 given area. These ecological processes may cause a shift in forest structure, which is
462 detected as a shift in the vertical structure signature by TLS or even HPs in sites with high
463 liana abundance. These differences in structures have been confirmed in a recent study,
464 which found that a liana-infested forest had a more irregular canopy with canopy heights
465 between 10 and 20 m, while the surrounding forests had a significantly taller canopy
466 between 25 and 35m along with a denser canopy (*Tymen et al., 2016*). Together, our results
467 and Tymen et al. (2016) observations could highlight the potential of entropy analysis of the
468 forests to detect the presence and the effect of lianas on the forest structure and the pathways
469 of succession.
470
471 **4.3 A cautionary tale associated to emergent TLS and HPs monitoring technologies**
472 **applied to liana-infested sites**
473 Our observations from changes on DBH_{mean}, TBA, PAI, $PAVD_{mean}$, LAI and canopy
474 openness as function of liana abundance provide evidence that these variables can be used to
475 estimate the impact of lianas on forest structure along the path of succession, although not
476 all of parameters, such as stem density and L/TBA, were significant. In other words, there is

a strong need to carefully select which parameters should be considered if we want to estimate changes in the forest structure as function of liana abundance. One key example is the use of PAI (PAI= LAI + Woody Area Index (WAI)) as tool to evaluate the impact of liana abundance on forest succession. PAI as a single measurement theoretically could provide insights on the impact of liana abundance on successional stages; as such we could expect that PAI will increase as leaf and wood biomass increases during succession (*Quesada et al., 2009*). Furthermore, PAI could be better understood if specific measurements of TLS can be done during the dry season to quantify the real value of WAI to PAI, tropical dry forests in contrast to tropical rainforests can provide significant advantage on better understanding PAI (Kalascka et al. 2005b). It is surprising that we did not find differences in the PAI values between stands that did and did not have lianas. It is possible that PAI is not the best parameter to differentiate between plots with and without liana presence, instead variables more related with leaf components, such as LAI and WAI may be more suitable for finding differences in liana signature across sites, especially when the contribution of lianas to the WAI to overall plot PAI is relatively small in comparison to the allocation of WAI from trees (*Kalascka et al. 2005b, Sanchez-Azofeifa et al., 2009*).

A recent study assessing the role of lianas on forest dynamics in the Amazon, indicated that a liana-infested forest appeared to be in an arrested stage of ecological succession, due to the evidence provided by LiDAR surveys from 2007 to 2012 which showed that the overall extent of forest area had remained stable, with no notable net gain or loss over the surrounding forest (*Tymen et al., 2016*). It is possible that studying forest dynamics in forest stands across successional stages, with different levels of liana abundance integrated into the TLS and HPs parameters, may allow us in the future to provide stronger

500 evidence as to whether lianas can arrest succession in dry forests as it appears to occur in
501 humid forests (*Schnitzer et al., 2000; Tymen et al., 2016*).
502 Moreover, our work seeks to strength the argument for the inclusion of lianas on
503 global terrestrial vegetation models (*Verbeek & Kearsley, 2016*). We argue here that the first
504 step on the development of such models is to have a clear understanding of how lianas affect
505 ecosystem structure and composition, which in turn, will affect tree mortality/recruitment,
506 and carbon storage aboveground and belowground (*Poulsen et al. 2016, Schnitzer et al.*
507 *2014*). Furthermore, lianas because of their impact on the 3D structure of a given forest
508 space, may have the possibility of changing faunal diversity (e.g. birds) an impact that has
509 not fully documented as today. As such, our study also supports the arguments by Schnitzer
510 et al (2016) that calls for the need for developing a network of observational and
511 experimental sites that can provide insights on the impact of lianas at different ecological
512 levels.
513 We extend the previous argument to remote sensing studies as well. Since lianas
514 represent a significant ecological component of tropical ecosystems (with stronger presence
515 on intermediate stages than early or late successional stages), we also argue that the
516 development of more robust global vegetation models must start from understanding liana
517 impact of forest structure which in turn will drive other components of those models.
518
519 **5 Conclusions**
520 This study evaluated the potential for TLS and hemispherical photos to observe differences
521 between successional stages of a tropical dry forest chrono-sequence and liana abundance.
522 Our work provided five main conclusions: (1) that TLS data combined with hemispherical

photography data can help to predict the forest structure of the tropical dry forest as demonstrated before, (2) that these predictions get blurry when liana abundance is considered, (3) that variations in TLS and HPs parameters can be used to predict the effect of liana abundance on the successional path, (4) that not all the parameters could address the effect of the presence or impact of lianas along a successional gradient, and (5) we suggest that the impact of lianas on successional stages changes the deterministic nature of forest structure, by randomizing the 3D space where they grow at given plot; the higher the abundance of lianas the higher the randomization.

Our study provides important insights on the contributions of lianas to the successional process, and highlights the potential that TLS and HPs have in monitoring liana presence in tropical dry forests environments. Lianas are increasing in density and biomass in tropical forests, but it is unknown whether this pattern is also found in secondary forests, which are suitable for liana proliferation. TLS systems, and to a lesser extent HPs are capable of providing unbiased estimations for the vertical structure of a given site, and thus constitute powerful tools to monitor the increases in liana density and biomass. Although, our study is limited to one single site in Costa Rica, this is a first step on the development of more comprehensive approaches, which take advantage of advanced technology to understand the effects of liana abundance on tropical dry forest structure. The approach presented in this paper, presents important contributions to efforts directed to estimate the potential effects of lianas on forest carbon in secondary forests (*Durán and Sanchez-Azofeifa, 2015*), elements that seems not fully considered yet in the tropical literature.

Acknowledgements

546 This work was carried out with the aid of a grant from the Inter-American Institute for
547 Global Change Research [IAI] CRN3 025 which is supported by the US National Science
548 Foundation [Grant GEO-1128040], and the Discovery Grant Program of the National
549 Science and Engineering Research Council of Canada. We thank Ericka James her help
550 during the process of data analysis. We thank also Dr. Stefan Schnitzer for comments on
551 earlier versions of the manuscript and the constructive comments from three anonymous
552 reviewers.

553

554 **References**

555 Arroyo-Mora, J.P., Sánchez-Azofeifa, G.A, Kalacska, M., Rivard, B., Calvo-Alvarado, J.,
556 and Janzen, D.: Secondary forest detection in a Neotropical dry forest landscape
557 using Landsat 7 ETM+ and IKONOS Imagery. Biotropica, 37(4), 497-507, 2005a.
558 Arroyo-Mora, J. P., Sanchez-Asofeifa, G.A, Rivard, B., Calvo-Alvarado, J. C. and Janzen,
559 D. H.: Dynamics in landscape structure and composition for the Chorotega region,
560 Costa Rica from 1960 to 2000, Agr. Ecosyst. Environ., 106(1), 27–39, 2005b.
561 Beland, M., Baldocchi, D. D., Widlowski, J.-L., Fournier, R. A. and Verstraete, M. M.: On
562 seeing the wood from the leaves and the role of voxel size in determining leaf area
563 distribution of forests with terrestrial LiDAR, Agr. Forest Meteorol., 184, 82–97,
564 2014.
565 Calvo-Alvarado, J., B McLennan, GA Sánchez-Azofeifa, and T Garvin.: Deforestation and
566 forest restoration in Guanacaste, Costa Rica: Putting conservation policies in context.
567 For. Ecol. Manage., 258(6), 931-940, 2009.

568 Canty, A. and Ripley B.: boot: bootstrap functions, available at: https://cran.r-
569 project.org/web/packages/boot/ (last access: September 30, 2016), 2016.
570 Cao, S., Yu, Q., Sanchez-Azofeifa, A., Feng, J., Rivard, B., & Gu, Z.: Mapping tropical dry
571 forest succession using multiple criteria spectral mixture analysis, ISPRS J.
572 Photogramm. Remote. Sens., 109, 17-29, 2015.
573 Castillo, M., Rivard, B., Sánchez-Azofeifa, A., Calvo-Alvarado, J. and Dubayah, R.: LIDAR
574 remote sensing for secondary Tropical Dry Forest identification, Remote Sens.
575 Environ., 121, 132–143, 2012.
576 Castro-Esau, K., Sánchez-Azofeifa, G.A. and Caelli, T.: Discrimination of lianas and trees
577 with leaf-level hyperspectral data, Remote Sens. Environ., 90(3), 353–372, 2004.
578 Chen, Y.-J., Bongers, F., Cao, K.-F. and Cai, Z.-Q.: Above- and below-ground competition
579 in high and low irradiance: tree seedling responses to a competing liana *Byttneria*
580 *grandifolia*, J. Trop. Ecol., 24, 517–524, 2008.
581 Clawges, R., Vierling, L., Calhoon, M. and Toomey, M.: Use of a ground-based scanning
582 lidar for estimation of biophysical properties of western larch (*Larix occidentalis*),
583 Int. J. Remote Sens. 28(19), 4331–4344, 2007.
584 Culvenor, D., Newnham, G., Mellor, A., Sims, N. and Haywood, A.: Automated In-Situ
585 Laser Scanner for Monitoring Forest Leaf Area Index, Sensors, 14(8), 14994–15008,
586 2014.
587 Dassot, M., Constant, T. and Fournier, M.: The use of terrestrial LiDAR technology in forest
588 science.: Application fields, benefits and challenges, Ann. For. Sci., 68(5), 959–974,
589 2011.

590 Dewalt, S. J., Schnitzer, S. A. and Denslow, J. S.: Density and diversity of lianas along a
591 chronosequence in a central Panamanian lowland forest, J. Trop. Ecol., 16(1), 1–19,
592 2000.
593 Durán, S.M. and Gianoli, E.: Carbon stocks in tropical forests decrease with liana density,
594 Biol. Lett., 3–6, 2013.
595 Durán, S. M. and Sánchez-Azofeifa.: Liana effects on carbon storage and uptake in mature
596 and secondary tropical forests, in: Biodiversity of lianas, edited by: Parthasarathy, N.,
597 pp. 43–55. Springer-Verlag, 2015.
598 Frazer, G.W., Canham, C.D., and Lertzman, K.P.: Gap light analyzer (GLA), Version 2.0:
599 Imaging software to extract canopy structure and gap light transmission indices from
600 true-colour fisheye photographs, users manual and program documentation. Simon
601 Fraser University, BC and the Institute of Ecosystem Studies, NY, 1999.
602 Foster, J. R., Townsend, P. A. and Zganjar, C. E.: Spatial and temporal patterns of gap
603 dominance by low-canopy lianas detected using EO-1 Hyperion and Landsat
604 Thematic Mapper, Remote Sens. Environ., 112 (5), 2104–2117, 2008.
605 González, I. and Déjean S.: CCA: canonical correlation analysis, available at: https://cran.r-
606 project.org/web/packages/CCA/ (last access: September 30, 2016), 2015.
607 Graham, E. A., Mulkey, S. S., Kitajima, K., Phillips, N. G. and Wright, S. J.: Cloud cover
608 limits net CO2 uptake and growth of a rainforest tree during tropical rainy seasons,
609 Proc. Natl. Acad. Sci. U. S. A., 100(2), 572–576, 2003.
610 van der Heijden, G.M.F, Schnitzer, S.A., Powers, J.S. and Phillips, O.L.: Liana impacts on
611 carbon cycling, storage and sequestration in tropical forests, Biotropica 45, 682–692,
612 2013.

van der Heijden, Powers, J.S., and Schnitzer, S.A.: Lianas reduce carbon accumulation and storage in tropical forests, PNAS, 112, 13267-13271, 2015.

Hilje, B., Calvo-alvarado, J., Jiménez-rodríguez, C., Sánchez-Azofeifa, A., José, S., Rica, C., Forestal, E. D. I., Rica, T. D. C. and Rica, C.: Tree species composition, breeding systems, and pollination and dispersal syndromes in three forest successional stages in a tropical dry forest in Mesoamerica, Trop. Conserv. Sci., 8(1), 76–94, 2015.

Jupp, D. L. B., Culvenor, D. S., Lovell, J. L., Newnham, G. J., Strahler, A. H. and Woodcock, C. E.: Estimating forest LAI profiles and structural parameters using a ground-based laser called "Echidna", Tree Physiol., 29(2), 171–81, 2009.

Kalacska, M.: Leaf area index measurements in a tropical moist forest: A case study from Costa Rica, Remote Sens. Environ., 91(2), 134–152, 2004.

Kalascka, M., J Calvo, and GA Sánchez-Azofeifa: Assessment of seasonal changes in species' leaf area in a tropical dry forest in different states of succession, Tree Physiol., 25: 733-744. 2005a.

Kalacska, M., Sánchez-Azofeifa, G. A., Calvo-Alvarado, J. C., Rivard, B. and Quesada, M.: Effects of season and successional stage on leaf area index and spectral vegetation indices in three mesoamerican tropical dry forests, Biotropica, 37(4), 486–496, 2005b.

Kalacska, M., Sanchez-Azofeifa, G. A., Rivard, B., Caelli, T., White, H. P. and Calvo-Alvarado, J. C.: Ecological fingerprinting of ecosystem succession: Estimating secondary tropical dry forest structure and diversity using imaging spectroscopy, Remote Sens. Environ., 108, 82–96, 2007a.

635 Kalacska, M., Bohlman, S., Sanchez-Azofeifa, G. A., Castro-Esau, K. and Caelli, T.:
636 Hyperspectral discrimination of tropical dry forest lianas and trees: Comparative data
637 reduction approaches at the leaf and canopy levels, Remote Sens. Environ., 109,
638 406–415, 2007b.
639 Ledo, A., Illian, J. B., Schnitzer, S. A., Wright, S. J., Dalling, J. W. and Burslem, D. F. R.
640 P.: Lianas and soil nutrients predict fine-scale distribution of above-ground biomass
641 in a tropical moist forest, J. Ecol., 104, 1819–1828, 2016.
642 Lefsky M., and McHale M..: Volumes estimates of trees with complex architecture from
643 terrestrial laser scanning, J. Appl. Remote. Sens., 2, 023521, 2008.
644 Letcher, S. G. and Chazdon, R. L.: Lianas and self-supporting plants during tropical forest
645 succession, For. Ecol. Manage., 257(10), 2150–2156, 2009.
646 Lovell, J. L., Jupp, D. L. B., Culvenor, D. S. and Coops, N. C.: Using airborne and ground-
647 based ranging lidar to measure canopy structure in Australian forests, Can. J. Remote
648 Sens., 29 (5), 607–622, 2014.
649 Menzel, U.: CCP: Significance tests for canonical correlation analysis (CCA), available at:
650 https://cran.r-project.org/web/packages/CCP/ (last access: September 30, 2016),
651 2012.
652 Muss, J. D., Aguilar-Amuchastegui, N., Mladenoff, D. J. and Henebry, G. M.: Analysis of
653 waveform lidar data using shape-based metrics, IEEE Geosci. Remote Sens. Lett.,
654 10(1), 106–110, 2013.
655 Paul, G. S. and Yavitt, J. B.: Tropical vine growth and the effects on forest succession: a
656 review of the ecology and management of tropical climbing plants, Bot. Rev., 77 (1),
657 11–30, 2010.

658 Phillips, O., Martínez, R., Arroyo, L. and Baker, T.: Increasing dominance of large lianas in
659 Amazonian forests, Nature, 418, 770–774, 2002.
660 Phillips, O. L. and Lewis, S. L.: Recent changes in tropical forest biomass and dynamics,
661 For. Glob. Chang., 4, 77–108, 2014.
662 Phillips, O. L., Vásquez Martínez, R., Monteagudo Mendoza, A., Baker, T. R. and Núñez
663 Vargas, P.: Large lianas are hyperdynamic elements of the tropical forest canopy,
664 Ecology, 86, 1250–1258, 2005.
665 Portillo-Quintero, C., Sanchez-Azofeifa, A. and Culvenor, D.: Using VEGNET In-Situ
666 monitoring LiDAR (IML) to capture dynamics of plant area index, structure and
667 phenology in Aspen Parkland Forests in Alberta, Canada, Forests, 5 (5), 1053–1068,
668 2014.
669 Poulsen, J. R., Koerner, S. E., Miao, Z., Medjibe, V. P., Banak, L. N. and White, L. J. T.:
670 Forest structure determines the abundance and distribution of large lianas in Gabon,
671 Glob. Ecol. Biogeogr., doi:10.1111/geb.12554, 2016.
672 Quesada, M., Sanchez-Azofeifa, G. A., Alvarez-Añorve, M., Stoner, K. E., Avila-Cabadilla,
673 L., Calvo-Alvarado, J., Castillo, A., Espírito-Santo, M. M., Fagundes, M., Fernandes,
674 G. W., Gamon, J., Lopezaraiza-Mikel, M., Lawrence, D., Morellato, L. P. C., Powers,
675 J. S., Neves, F. D. S., Rosas-Guerrero, V., Sayago, R. and Sanchez-Montoya, G.:
676 Succession and management of tropical dry forests in the Americas: review and new
677 perspectives, For. Ecol. Manage., 258 (6), 2009.
678 Quinn, G. P. and Keough M. J.: Experimental Design and Data Analysis for Biologists.
679 Cambridge University Press, New York, 443-472, 2002.

680 R Development Core Team: R: a language and environment for statistical computing,
681 available at: http://www.r-project.org (last access: September 30, 2016), 2016.
682 Ramírez, F. A., Armitage, R. P. and Danson, F. M.: Testing the application of terrestrial
683 laser scanning to measure forest canopy gap fraction, Remote Sens., 5 (6), 3037–
684 3056, 2013.
685 Richardson, J., Moskal, L. and Bakker, J.: Terrestrial laser scanning for vegetation sampling,
686 Sensors, 14(11), 20304–20319, 2014.
687 Sánchez-Azofeifa, RC Harris, and DL Skole. Deforestation in Costa Rica: a quantitative
688 analysis using remote sensing imagery. Biotropica. 33(3), 378-384, 2001.
689 Sánchez-Azofeifa, G. A. and Castro-Esau, K.: Canopy observations on the hyperspectral
690 properties of a community of tropical dry forest lianas and their host trees, Int. J.
691 Remote Sens., 27 (10), 2101–2109, 2006.
692 Sánchez-Azofeifa, G. A., Kalácska, M., Espírito-Santo, M. M. Do, Fernandes, G. W. and
693 Schnitzer, S.: Tropical dry forest succession and the contribution of lianas to wood
694 area index (WAI), For. Ecol. Manage., 258 (6), 941–948, 2009.
695 Schnitzer, S. A and Bongers, F.: Increasing liana abundance and biomass in tropical forests:
696 emerging patterns and putative mechanisms, Ecol. Lett., 14(4), 2011.
697 Schnitzer, S. A and Carson, W. P.: Lianas suppress tree regeneration and diversity in treefall
698 gaps, Ecol. Lett., 13 (7), 849–57, 2010.
699 Schnitzer, S. A., Dalling, J. W. and Carson, W. P.: The impact of lianas on tree regeneration
700 in tropical forest canopy gaps: evidence for an alternative pathway of gap-phase
701 regeneration, J. Ecol., 88 (4), 655–666, 2000.

Schnitzer, S., van der Heijden, G.M.F., and Powers, J.: Addressing the challenges of including lianas in global vegetation models, PNAS, 113 (1), E6, 2016.

Schnitzer, S. A., van der Heijden, G., Mascaro, J. and Carson, W. P.: Lianas in gaps reduce carbon accumulation in a tropical forest, Ecology, 95, 3008–3017, 2014.

Strahler, A. H., Jupp, D. L. ., Woodcock, C. E., Schaaf, C. B., Yao, T., Zhao, F., Yang, X., Lovell, J., Culvenor, D., Newnham, G., Ni-Miester, W. and Boykin-Morris, W.: Retrieval of forest structural parameters using a ground-based lidar instrument (Echidna ®), Can. J. Remote Sens., 34 (sup2), S426–S440, 2014.

Tymen, B., Réjou-Méchain, M., Dalling, J. W., Fauset, S., Feldpausch, T. R., Norden, N., Phillips, O. L., Turner, B. L., Viers, J. and Chave, J. Evidence for arrested succession in a liana-infested Amazonian forest, J. Ecol., 104 (1), 149-159. 2016.

Verbeek, H., Kearsley, E.: The importance of including lianas in global vegetation models, PNAS, 113 (1), E4, 2016.

Wright, S. J.: Tropical forests in a changing environment, Trends Ecol. Evol., 20(10), 553–560, 2005.

Zhang, J., Rivard, B., Sánchez-Azofeifa, A. and Castro-Esau, K.: Intra- and inter-class spectral variability of tropical tree species at La Selva, Costa Rica: Implications for species identification using HYDICE imagery, Remote Sens. Environ., 105, 129–141, 2006.

722 Table 1. Mean (± SD) of parameters of forest structure extracted from plots with
723 different successional stages and different relative abundance of lianas in the dry forest
724 at Santa Rosa National Park, Costa Rica. Significant differences (*F-values* and their *p-*
725 *values*) according to the successional stages, relative abundance of lianas and their
726 interaction are represented by a posteriori ANOVA text extracted from MANOVA. Stem
727 density (stems/ha); DBH_{mean}, mean stem diameter at breast height (cm); TBA, total basal
728 area (m^2); L/TBA, ratio of liana basal area to TBA.

Parameters	Early		Intermediate		ANOVA		
	LL	HL	LL	HL	Stage	Condition	Interaction
Stem density	1054 ± 370.72	1218.33 ± 603.24	1027.14 ± 379.02	1021 ± 331.54	0.55	0.15	0.27
DBH_{mean}	10.91 ± 2.36	11.83 ± 1.57	14.17 ± 1.85	11.56 ± 1.89	2.72	2.73	5.65*
TBA	1.44 ± 0.90	2.08 ± 1.01	2.61 ± 0.80	1.84 ± 0.61	1.39	0.48	5.15*
L/TBA (10^{-2})	0.38 ± 0.35	1.48 ± 0.84	0.35 ± 0.32	2.93 ± 2.14	2.76	14.11***	1.86

729 *, $p < 0.05$; ***, $p < 0.01$

730

731 Table 2. Mean (± SD) of parameters calculated by VEGNET system and HPs in plots
732 with different successional stages and different relative abundance of lianas in the dry
733 forest at Santa Rosa National Park, Costa Rica. Significant differences (*F-values* and
734 their *p-values*) according to the successional stages, relative abundance of lianas and
735 their interaction are represented by a posteriori ANOVA text extracted from MANOVA.
736 RG, radius of gyration; PAI, plant area index; $PAVD_{mean}$, plant area volume density;
737 H_{max}, maximum tree height (m); LAI, leaf area index.

Parameters	Early		Intermediate		ANOVA		
	LL	HL	LL	HL	Stage	Condition	Interaction
RG	4.21 ± 1.42	4.85 ± 0.92	4.69 ± 1.11	4.34 ± 0.91	0.03	0.01	1.41
C_x	0.19 ± 0.06	0.13 ± 0.04	0.14 ± 0.03	0.16 ± 0.04	0.12	0.14	5.95*
C_y	7.56 ± 2.96	8.43 ± 1.63	8.22 ± 2.07	7.56 ± 1.59	0.07	0.01	0.96
PAI	2.45 ± 0.28	2.10 ± 0.28	2.13 ± 0.34	2.31 ± 0.33	0.06	0.05	4.75*
$PAVD_{mean}$	0.19 ± 0.05	0.13 ± 0.04	0.14 ± 0.03	0.16 ± 0.04	0.14	0.22	7.26*
H_{max}	17.42 ± 5.51	18.17 ± 3.90	23.26 ± 7.73	18.01 ± 6.00	0.99	1.53	1.61
LAI	2.30 ± 0.32	2.46 ± 0.64	2.34 ± 0.46	2.92 ± 0.39	2.97	6.91*	1.32
Canopy openness	13.90 ± 3.94	12.59 ± 5.89	12.74 ± 5.27	8.67 ± 1.47	5.77*	6.78*	0.79

738 *, $p < 0.05$

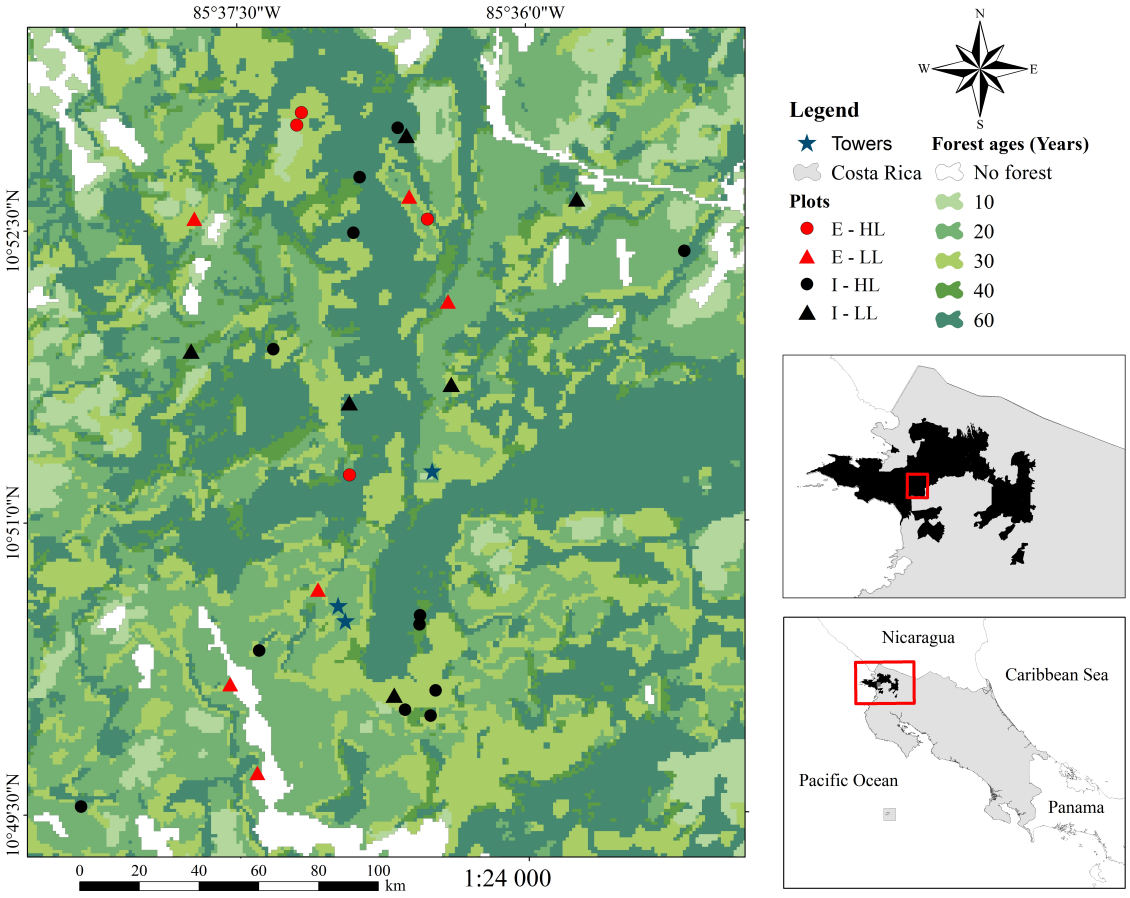

Figure 1. Location of the sampled forest plots at the Santa Rosa National Park Environmental Monitoring Super Site, Guanacaste, Costa Rica. Where E-HL indicates Early successional stage with a high relative abundance of lianas; E-LL Early successional stage with a low relative abundance of lianas; I-HL, Intermediate successional stage with a high relative abundance of lianas; I-LL, Intermediate successional stage with a low relative abundance of lianas. In addition, forests ages refer to: 60, forests detected since 1956; 40, forests detected since 1979; 30, forests detected since 1986; 20, forests detected since 1997; 10 forests detected since 2005, and no forest correspond to non-related to woodlands.

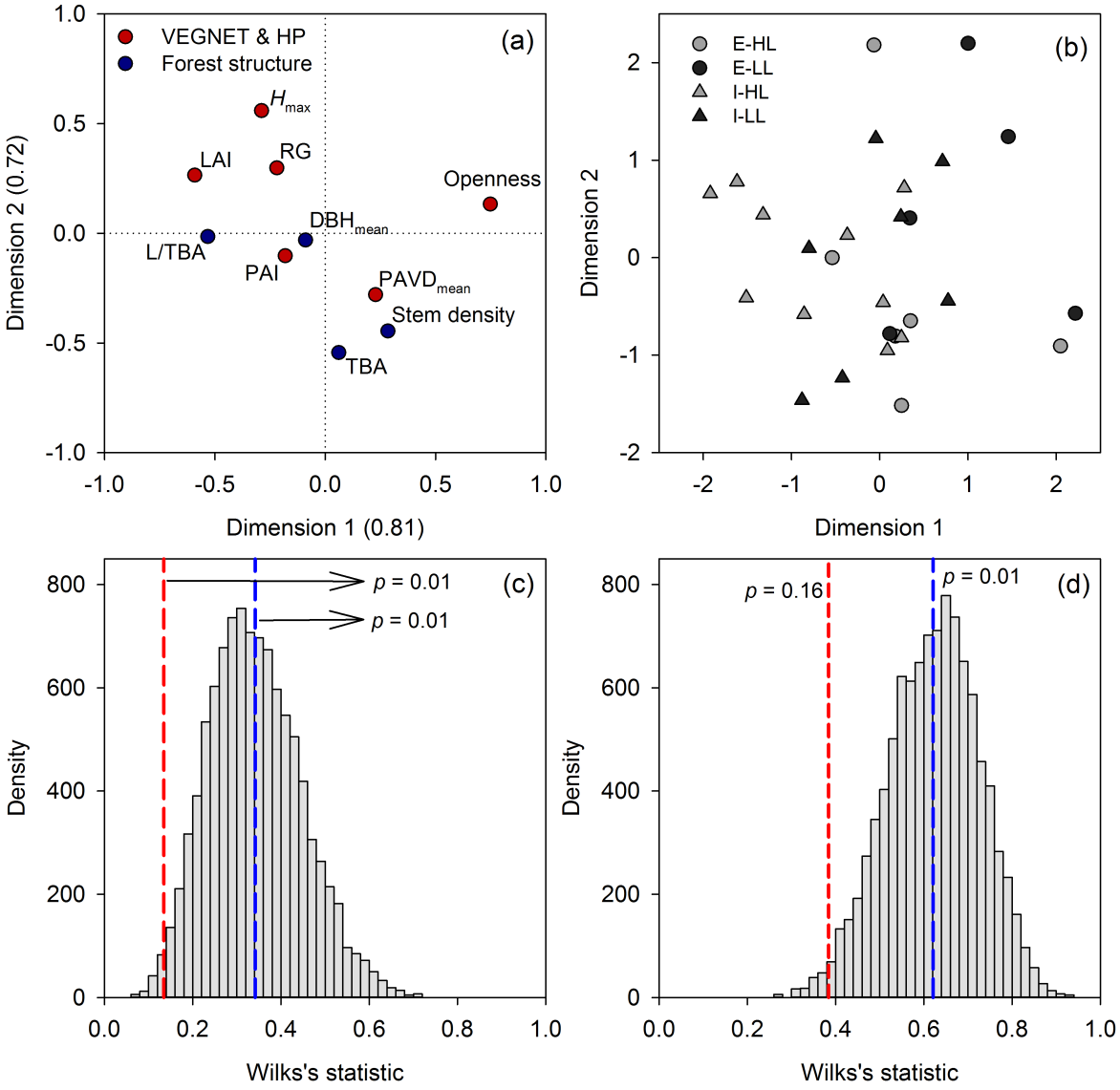

752

753 Figure 2. Canonical correspondence analysis to describe the association between the
754 parameters estimated by VEGNET system-hemispherical photographs (HPs) and the
755 forest structure. a) VEGNET-HPs coefficients are represented by red points, while forest
756 structure coefficients are represented by blue points. b) Individual scores of each plot of
757 the canonical variates are represented according to successional stages (E, early; I,
758 intermediate) and relative liana abundance (LL, low liana abundance; HL, high liana
759 abundance). C and d represent the permutation distribution of the Wilks' Lambda test to

760 assign the statistical significance of canonical correlation coefficients considering 4 and
761 3 canonical correlations, respectively; the red line represent the original value Wilks'
762 Lambda, while the blue line represent the mean value permutated. The *p* values next to
763 each line represent the significance of the Wilks' Lambda test.
764

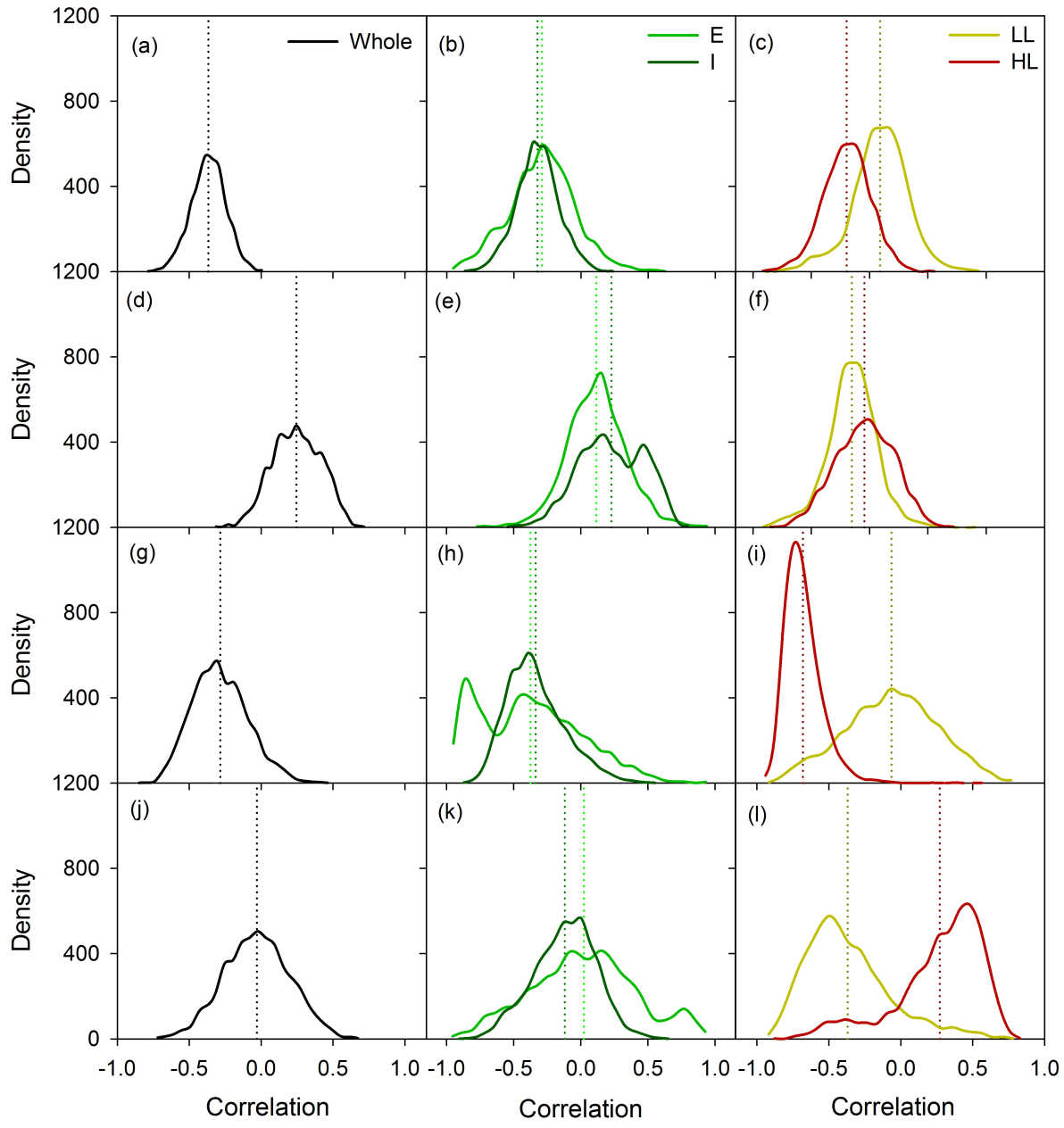

765

766 Figure 3. Density distribution of the bootstrapped correlation coefficients without and
767 with distinction between successional stages (E, early; I, intermediate) and relative liana
768 abundance (LL, low liana abundance; HL, high liana abundance). a, b, and c correspond
769 to the correlation of canopy openness and the ratio of liana basal area to total basal area
770 (L/TBA); d, e, f correspond to leaf area index-L/TBA correlation; g, h, and i correspond
771 to the maximum tree height-TBA correlation; j, k, and l correspond to plant area volume

772 density-TBA correlation. Each dotted line represents the mean value of the bootstrapped
773 correlation.